Nanoscale

COMMUNICATION

View Article Online
View Journal | View Issue



Cite this: *Nanoscale*, 2018, **10**, 20514

Received 4th August 2018,
Accepted 27th October 2018

DOI: 10.1039/c8nr06283h

rsc.li/nanoscale



# Boron based nanosheets as reducing templates in aqueous solutions: towards novel nanohybrids with gold nanoparticles and graphene†

Asha Liza James, [a] Shikha Khandelwal, [b] Arnab Dutta [b] and Kabeer Jasuja *[a]

**We show that nanosheets obtained by exfoliating magnesium diboride bear an intrinsic ability to elicit chemical reduction of quinone-based molecules. They also reduce gold salt into ultra-small gold nanoparticles and graphene oxide into reduced graphene oxide. These nanosheets subsequently interface with the partner nanomaterial in solution to form novel nanohybrids.**

Two-dimensional (2D) forms of boron have started receiving significant attention over the last few years. Several theoretical studies in the past had predicted the structures, stability, as well as feasibility of synthesising boron sheets.[1] The actual experimental realisation, however, was achieved only recently through chemical vapour deposition, which resulted in 2D boron films on copper foil.[2] Since then, several bottom-up approaches involving growth on metallic substrates have been reported.[3–5] There has also been a growing interest in identifying top-down approaches that can produce quasi-2D forms of boron.[6] This is especially evident from the recent studies on exfoliation of layered metal borides – a class of compounds that inherently contain (graphene-like) honeycomb boron planes interleaved with metal atoms (Fig. 1a).[7–9] For example, it has been shown that exfoliation of layered magnesium boride ($MgB_2$) can be achieved by utilising ultrasonication,[7,10] chelation,[8] or cation exchange.[11] It is pertinent to note that the nanosheets obtained through these approaches are found to contain boron planes chemically modified with functional groups.

In this work, we firstly demonstrate that the nanosheets derived from $MgB_2$ bear an intrinsic ability to elicit a chemical reduction reaction in an aqueous medium. Secondly, we show that these nanosheets can reduce specific quinone-based molecules to quinols, gold salt into ultra-small gold nanoparticles, and graphene oxide (GO) into reduced graphene oxide (rGO). Finally, we show that subsequent to causing reduction, the boron based nanosheets also interface with the partner nanomaterial to form novel nanohybrids. This is of immense practical merit considering that while newer 2D materials are being discovered, there is also a surging interest in combining these with other nano-dimensional materials to create heterostructures which exhibit a synergistic blend of the constituent properties.[12]

Boron based nanosheets were obtained in the form of an aqueous dispersion by carrying out the chemical exfoliation of layered $MgB_2$ (Fig. 1a and b; experimental details in section 1, ESI†).[8] We found these nanosheets to exhibit complex boron hydrides and oxy functional groups as confirmed by solid-state $^{11}B$ NMR spectroscopy (Fig. S1, ESI†). We postulated whether these functional groups could endow a chemically reducing character to the nanosheets because borohydrides (like

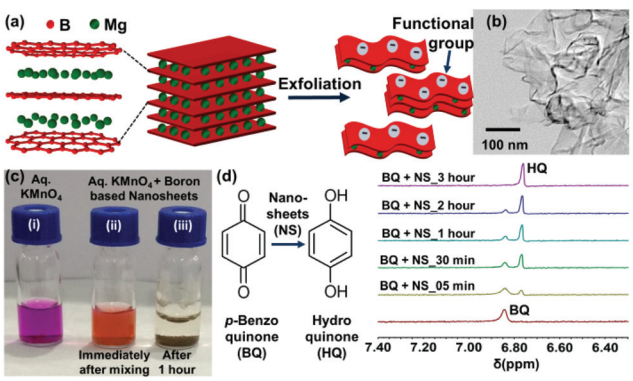


**Fig. 1** (a) Layered magnesium diboride is chemically exfoliated into boron based nanosheets; (b) TEM image of a nanosheet; (c) reducing action on $KMnO_4$: (i) purple $KMnO_4$ solution turns into (ii) reddish-orange solution upon adding an aqueous dispersion of boron-based nanosheets and finally forms (iii) a brown precipitate of $MnO_2$; (d) nanosheets mediated reduction of *p*-benzoquinone into hydroquinone as monitored by $^1H$ solution NMR.

[a]*Discipline of Chemical Engineering, Indian Institute of Technology, Gandhinagar, Gujarat 382355, India. E-mail: kabeer@iitgn.ac.in*
[b]*Discipline of Chemistry, Indian Institute of Technology, Gandhinagar, Gujarat 382355, India. E-mail: arnab.dutta@iitgn.ac.in*

†Electronic supplementary information (ESI) available: Detailed experimental methods, movies depicting chemical reactions and additional microscopic and spectroscopic characterization. See DOI: 10.1039/c8nr06283h

$NaBH_4$) are conventionally used as strong reducing agents in synthetic chemistry. To obtain a preliminary insight, we first observed the reaction of nanosheet dispersion with a strong oxidising agent, namely potassium permanganate ($KMnO_4$).

Upon mixing the colourless dispersion of nanosheets with a purple coloured aqueous solution of $KMnO_4$, a rapid colour change to reddish orange was observed. This solution gradually turned yellow and eventually formed a brown precipitate of $MnO_2$ (Fig. 1c and Movie S1, ESI†). Such gradual and stepwise reduction steps are not discernible when $KMnO_4$ is reduced by $NaBH_4$ (Movie S2, ESI†). The reaction was also monitored spectrophotometrically to develop a quantitative understanding of the kinetics (Fig. S2†).

The ability of nanosheets to reduce $KMnO_4$ in a gradual manner encouraged us to explore their chemical reactivity towards organic molecules. For these experiments, quinone compounds were chosen because (i) borohydride compounds typically facilitate reduction of carbonyl groups in aldehydes and ketones, and (ii) quinone-quinol compounds are well established redox systems. *p*-Benzoquinone was selected as the first candidate owing to its feasibility to be reduced by $NaBH_4$. The interaction of nanosheets with *p*-benzoquinone was monitored using UV-Vis and $^1H$ solution NMR spectroscopy (section S1, ESI†). The nanosheets were indeed found to reduce *p*-benzoquinone into hydroquinone (Fig. 1d and S3, 4, ESI†). Similarly, we found that an *o*-benzoquinone derivative, namely 3,5-di-*tert*-butyl-*o*-benzoquinone, could also be reduced by the nanosheets (Fig. S5, ESI†). However, we found that the nanosheets were not able to reduce other quinone derivatives, namely anthraquinone and 9,10-phenanthraquinone, even after 15 hours of interaction (Fig. S6 and 7, ESI†). The nanosheets could not elicit the reduction of benzil as well (Fig. S8, ESI†). These observations suggest that the boron based nanosheets can reduce only a select range of compounds. We identified that the compounds which could be reduced by the nanosheets have a standard reduction potential >0.16 V (*versus* SHE) in neutral aqueous medium (as summarised in Fig. 2a). This is in contrast to $NaBH_4$ that can reduce all the tested compounds (including benzil, that has a reduction potential of −0.44 V *versus* SHE).

Such a gradual reduction compared to $NaBH_4$ can be attributed to the nature of hydride species possessed by the nanosheets. The $^{11}B$ solid-state NMR spectrum shows the presence of at least two different hydride species – $[B_{12}H_{12}]^{2-}$ and $[B_3H_8]^-$, which are expected to be milder in reducing activity compared to naked $BH_4^-$ (Fig. S1, ESI†).[13] Furthermore, because these species are structurally integrated to the nanosheets, their activity also depends on the diffusional effects. These nanosheets present an avenue to harness the reducing properties of borohydrides in a controlled and gradual manner. Being comparatively mild in reactivity, these can provide a better synthetic control when compared to other reactive hydride reagents such as $NaBH_4$ or $LiAlH_4$.[14,15] The selective reduction of specific quinone-based ketone groups by the nanosheets also points to an ability that may be tuned towards developing a new class of slow acting reducing agents.

The concurrence of reducing nature and quasi-two dimensionality imparts these boron based nanosheets an unprecedented ability – to act as reactive templates onto which another nanodimensional system could be integrated *via in situ* reduction. Such a nanoscale integration would enable multiple functionalities within an ultra-small packet, which could be chemically and/or catalytically active. There is also a rising interest in developing nanoscaled heterostructures by interfacing two or more distinct nano-dimensional materials. Such hybrid nanostructures exhibit a range of new properties owing to the presence of several novel interfaces, which are otherwise challenging to realize.[16] This motivated us to investigate if the nanosheets can be incorporated as an active reagent in the synthesis of gold nanoparticles. The rationale behind this being the fact that recipes for synthesis of gold nanoparticles conventionally employ a reduction of the gold salt by sodium borohydride in the presence of stabilizing agents.[17] We hypothesized that the boron based nanosheets would not only reduce the gold salt; these would also stabilize the as-formed gold nuclei by providing these a favourable template to anchor upon. Several studies have established the potential of nanosheets to stabilise nanoparticles on account of their high interfacial area and functional groups.[18]

We found that a simple addition of the yellow gold salt ($HAuCl_4{\cdot}3H_2O$) solution into the colourless aqueous dispersion of boron based nanosheets instantaneously resulted in a reddish brown coloured colloid (inset Fig. 2b, Movie S3, and experimental details in ESI†). UV-vis spectrum of the resultant colloid was found to exhibit a broad absorbance peak at ~510 nm, compared with nanosheets that exhibit a featureless spectrum in the visible region (Fig. 2b). The occurrence of this new peak indicates the formation of gold nanoparticles, the presence of which was confirmed by TEM analysis. TEM images revealed that not only had the nanoparticles (with dimensions <10 nm) formed, these had also anchored onto the nanosheets resulting in gold nanoparticle (AuNP)-nanosheet hybrids (Fig. 3a–c). STEM-elemental mapping of the nanohybrids depicted in Fig. 3d clearly indicates the presence of gold on the boron based nanosheets. Additional TEM and HRTEM images, EELS analysis, size distribution, and AFM images of these nanohybrids can be found in ESI (Fig. S9–S12†).

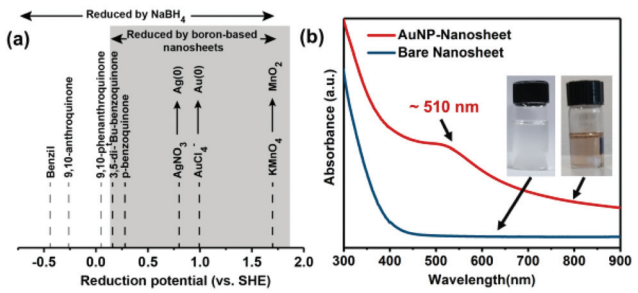


**Fig. 2** (a) Comparing the reducing potential of boron based nanosheets with $NaBH_4$; (b) UV-Vis spectra of bare nanosheets and AuNP-nanosheets.

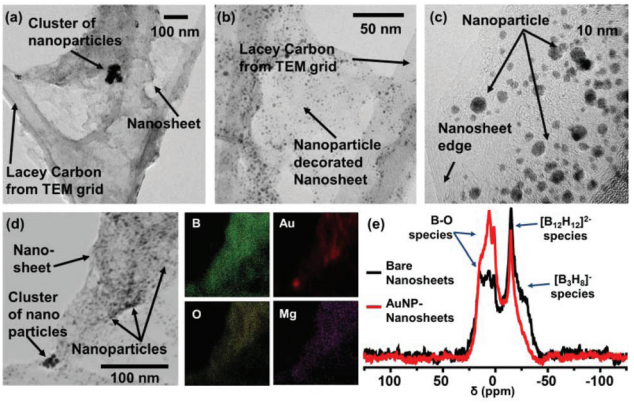


**Fig. 3** (a–c) HR-TEM images of the AuNP-nanosheets; (d) STEM-elemental maps showing boron, gold, oxygen, and magnesium. (e) Comparing $^{11}$B solid state NMR spectra of bare and gold nanoparticle decorated nanosheets.

To understand the chemical state of boron in the nanohybrids, solid-state $^{11}$B NMR spectrum was obtained from the lyophilised form of dispersions (Fig. 3e). The nanohybrids were found to display a less intense boron hydride peak relative to that of the oxy functional groups, when compared with bare nanosheets. The $^{11}$B NMR data also suggests that the reduction was primarily led by the $[B_3H_8]^-$ species while the $[B_{12}H_{12}]^{2-}$ species played a secondary role.[13] A similar decrease in the B–H functional groups in the nanohybrids was also evident in the FTIR spectra (Fig. S13, ESI†). Another observation supporting the borohydride-mediated reduction was a gain in the intensity of the B–O and B–OH bands in the nanohybrids. This increase can be attributed to the fact that the borohydrides, upon reduction, convert into boric acid or borate compounds.[19] These findings were also corroborated by the B 1s and Au 4f spectra obtained from the X-ray Photoelectron Spectroscopy (XPS) analysis of the nanohybrids. While the B 1s spectrum displayed a prominent peak corresponding to highly oxidised boron, the Au 4f spectrum exhibited peaks at 84.05 eV (Au $4f_{7/2}$) and 87.85 eV (Au $4f_{5/2}$) corresponding to the metallic state of gold ($Au^0$) confirming the reduction of gold salt (Fig. S14 and 15, ESI†).[20]

The typical sizes of gold nanoparticles formed by borohydride mediated reduction are also <10 nm, which is in accordance with our observations (Fig. 3c and S11, ESI†). It is pertinent to note that in this methodology no additional chemical was needed as a reducing agent. This is in contrast to conventional protocols where metallic nanoparticle-nanosheet composites are synthesised by the reduction of metal salts using reagents like sodium borohydride, ethylene glycol, sodium citrate, ascorbic acid, amines *etc.*[21] Such an intrinsic reducing capability to form stable gold nanoparticles has also been reported recently for a boron cluster $[closo\text{-}B_{12}H_{12}]^{2-}$.[22] Also, the reduction happens spontaneously and does not need any additional aide like sonication or thermal treatment.

Raman spectroscopy of the nanohybrids suggested the possible existence of a chemical interface. The Raman signal of nanosheets was found to be enhanced ~16 fold in the presence of nanoparticles (Fig. S16†). Enhancement factors <100 are generally associated with chemical interaction at the nanoparticle interface, involving charge transfer complexes.[23] We were also able to achieve a similar reduction of two other noble metal salts (silver nitrate and chloroplatinic acid hexahydrate) to obtain silver nanoparticle and platinum nanoparticle decorated nanosheet hybrids (Fig. S17†).

The ability of these nanosheets to effect *in situ* reduction and subsequently interface with the formed nanoparticles (0D–2D hybrid) led us to explore if this phenomenon can also be utilised to reduce graphene oxide dispersions to realise a novel boron-graphene nano construct (2D–2D hybrid). We investigated this possibility by mixing boron based nanosheets in aqueous dispersions of graphene oxide (GO) for a sufficient time (experimental details in ESI†). We observed that upon adding boron based nanosheets, the yellowish brown GO dispersion gradually turns darker in colour and eventually settles down as dark black sediments suggesting reduction (Fig. 4a). The sediment was re-dispersed in water using sonication and analysed by UV-Vis spectroscopy (Fig. 4b). While the GO dispersion shows a primary peak near 230 nm that corresponds to $\pi \rightarrow \pi^*$ transitions, the primary peak in the re-dispersed sample was found to be shifted to higher wavelengths. Such a red shift indicates restoration of the $sp^2$ network of C atoms and validates the reduction of GO.[24]

TEM imaging of the sediments reveal nanostructures that are heavily crumpled and consist of many entangled sheets, as depicted in Fig. 4c–g. This suggests that boron based nanosheets have likely formed a hybrid with the reduced GO (rGO). This was supported by the elemental mapping and EELS (Fig. S18 and 19, ESI†) of these samples, which depict the co-existence of both boron and carbon. It is pertinent to note that as these two elements are row neighbours in the periodic table, TEM imaging lacks sufficient contrast to clearly distinguish between graphene and boron based nanosheets. Also, detecting boron while carbon is present in excess is challenging. To address this, we utilized the presence of Mg as an indication of the boron based sheets in the elemental maps of the nanohybrids (as the chemical exfoliation of $MgB_2$ also leaves some amount of Mg in the boron based nanosheets).[8] Similar insights were also gained from the FE-SEM imaging of the hybrids (Fig. S20–23†).

XPS analysis of the nanohybrids also reveals a partial restoration of the C–C bonds when compared with GO due to the reduction of C–O groups (Fig. 4h and i). Typically, the deconvoluted C 1s spectra from GO and its derivatives exhibit three main daughter peaks corresponding to C–C (284.5 eV), C–O (286.6 eV), and C═O (288.5 eV) bonds. The rGO hybrids were observed to have higher peak intensity for C–C component and lower peak intensity for C–O component as compared with GO, confirming that boron based nanosheets were able to partially reduce graphene oxide.[25]

We obtained further insights on the degree of graphene oxide reduction by comparing the D and G bands in the Raman spectra. While the G band is attributed to the $E_{2g}$

 

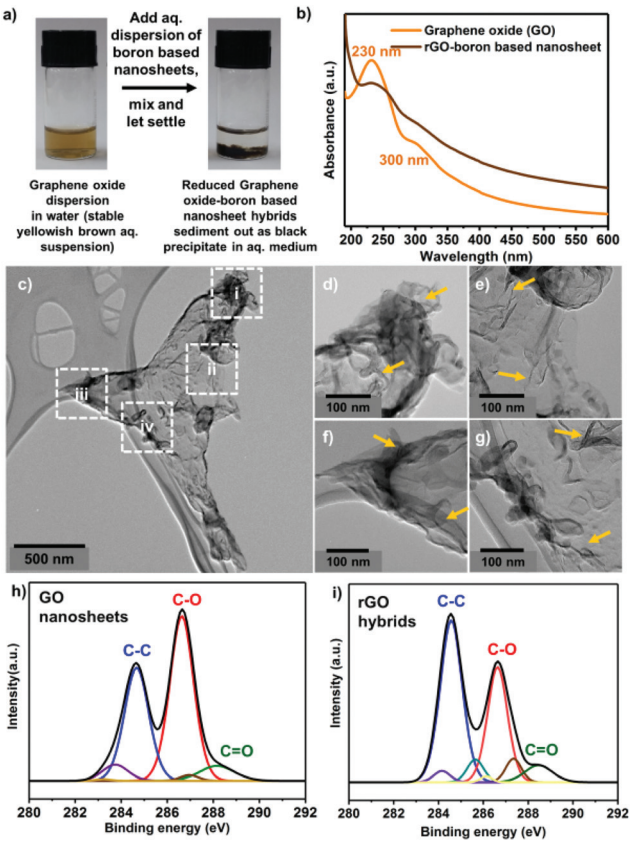


**Fig. 4** Reduction of graphene oxide to form rGO-boron based nanosheet hybrids: (a) schematic representing the reduction process; (b) UV-Vis spectra of GO and rGO dispersions; (c–g) TEM images of rGO-boron based nanosheet hybrids. Marked regions (i)–(iv) in (c) are zoomed in and depicted as the subsequent images (d)–(g) respectively. It may be noted that multiple layers (indicated by arrows) are present in the highly crumpled regions indicating the presence of two or more nanosheets. (h) C 1s spectra of GO and (i) rGO-Boron based nanosheet hybrid.

mode (in-plane stretching vibrations) of $sp^2$ carbon atoms, the D band is associated with structural defects, edge effects, and partially disordered structures of the $sp^2$ domains. The D and G bands in the Raman spectra of rGO-boron hybrids were found to be shifted to lower wavenumbers, 1350 and 1575 $cm^{-1}$, as compared with those in GO, at 1354 and 1584 $cm^{-1}$ (Fig. S24†). This is characteristic to the reduction of GO as reported in the literature.[25] The rGO-boron based nanosheet hybrids were found to have an $I_D/I_G$ ratio of 0.953 compared with $I_D/I_G$ ratio of 0.902 observed in GO, supporting partial reduction.

The creation of such an interface between low dimensional forms of boron and carbon warrants special attention in the purview of the current trend to develop novel heterostructures, wherein considerable efforts have been dedicated to interface graphene with other 2D materials like boron nitride, $MoS_2$, and even phosphorene.[26] Recent theoretical studies have also predicted the interface of borophene with several 2D materials including graphene towards "boro/2D semiconductor heterostructures".[27] Moreover, boron doping of graphene derivatives is an actively researched area because it has been shown to induce distinctive changes in the chemical and electrical properties of graphene.[28] Hence, a 2D boron–carbon hybrid is a particularly curious system to attain and explore for the plethora of modified properties it may exhibit. To the best of our knowledge, the work reported here is the first experimental report on interfacing boron based nanosheets with graphene to form a boron–carbon quasi 2D hybrid in aqueous solution. This approach holds the potential to be developed as a new technique to assemble colloidal nanosheets towards forming 'heterostructures in liquid'.[29]

## Conclusion

In summary, the capability of these nanosheets to act as chemically reducing agents unveils a relatively unexplored facet offered by the landscape of 2D materials. The formation of nanohybrids with gold and graphene provides the proof of concept that the inherent reducing character of these nanosheets can be availed to create diverse mixed-dimensional heterostructures in solution. The resultant nanohybrids hold immense potential in the pursuit to develop multi-functional materials. Our initial experiments indicate that the noble metal nanoparticle-nanosheet hybrids are excellent electrocatalysts for hydrogen evolution reaction (preliminary data presented in Fig. S25†). We expect that a detailed elucidation of the mechanisms underlying the reducing action of these nanosheets would enable a rational incorporation of these nanomaterials in a broad spectrum of applications, especially in supercapacitors, plasmonics, hydrogen storage, catalysis, and sensing.

## Conflicts of interest

There are no conflicts to declare.

## Acknowledgements

This work was supported by seed funding from IIT Gandhinagar; INSPIRE Faculty Award Research Grant (DST/INSPIRE/04/2014/001601) and Core Research Grant (EMR/2015/002462 and EMR/2017/000730) by the Department of Science and Technology, India.

## Notes and references

1 Y. Liu, E. S. Penev and B. I. Yakobson, *Angew. Chem., Int. Ed.*, 2013, **52**, 3156–3159.
2 G. Tai, T. Hu, Y. Zhou, X. Wang, J. Kong, T. Zeng, Y. You and Q. Wang, *Angew. Chem., Int. Ed.*, 2015, **54**, 15473–15477.
3 Z. Zhang, E. S. Penev and B. I. Yakobson, *Chem. Soc. Rev.*, 2017, **46**, 6746–6763.

4 B. Feng, J. Zhang, Q. Zhong, W. Li, S. Li, H. Li, P. Cheng, S. Meng, L. Chen and K. Wu, *Nat. Chem.*, 2016, **8**, 563.
5 A. J. Mannix, X.-F. Zhou, B. Kiraly, J. D. Wood, D. Alducin, B. D. Myers, X. Liu, B. L. Fisher, U. Santiago, J. R. Guest, M. J. Yacaman, A. Ponce, A. R. Oganov, M. C. Hersam and N. P. Guisinger, *Science*, 2015, **350**, 1513–1516.
6 T. Kondo, *Sci. Technol. Adv. Mater.*, 2017, **18**, 780–804.
7 S. K. Das, A. Bedar, A. Kannan and K. Jasuja, *Sci. Rep.*, 2015, **5**, 10522.
8 A. L. James and K. Jasuja, *RSC Adv.*, 2017, **7**, 1905–1914.
9 C. S. Lim, Z. Sofer, V. Mazanek and M. Pumera, *Nanoscale*, 2015, **7**, 12527–12534.
10 H. Nishino, T. Fujita, A. Yamamoto, T. Fujimori, A. Fujino, S.-i. Ito, J. Nakamura, H. Hosono and T. Kondo, *J. Phys. Chem. C*, 2017, **121**, 10587–10593.
11 H. Nishino, T. Fujita, N. T. Cuong, S. Tominaka, M. Miyauchi, S. Iimura, A. Hirata, N. Umezawa, S. Okada, E. Nishibori, A. Fujino, T. Fujimori, S.-i. Ito, J. Nakamura, H. Hosono and T. Kondo, *J. Am. Chem. Soc.*, 2017, **139**, 13761–13769.
12 A. T. S. Wee, M. C. Hersam, M. Chhowalla and Y. Gogotsi, *ACS Nano*, 2016, **10**, 8121–8123.
13 A. Remhof, Y. Yan, D. Rentsch, A. Borgschulte, C. M. Jensen and A. Zuttel, *J. Mater. Chem. A*, 2014, **2**, 7244–7249.
14 M. R. Johnson and B. Rickborn, *J. Org. Chem.*, 1970, **35**, 1041–1045.
15 M. V. N. d. Souza and T. R. A. Vasconcelos, *Appl. Organomet. Chem.*, 2006, **20**, 798–810.
16 D. Jariwala, T. J. Marks and M. C. Hersam, *Nat. Mater.*, 2016, **16**, 170.
17 C. Deraedt, L. Salmon, S. Gatard, R. Ciganda, R. Hernandez, J. Ruiz and D. Astruc, *Chem. Commun.*, 2014, **50**, 14194–14196.
18 P. T. Yin, S. Shah, M. Chhowalla and K.-B. Lee, *Chem. Rev.*, 2015, **115**, 2483–2531.
19 G. N. Glavee, K. J. Klabunde, C. M. Sorensen and G. C. Hadjapanayis, *Langmuir*, 1992, **8**, 771–773.
20 P. Tripathy, A. Mishra, S. Ram, H. J. Fecht, J. Bansmann and R. J. Behm, *Nanotechnology*, 2009, **20**, 075701.
21 C. Tan, X. Huang and H. Zhang, *Mater. Today*, 2013, **16**, 29–36.
22 B. Qi, C. Wu, L. Xu, W. Wang, J. Cao, J. Liu, S. Zhang, D. Gabel, H. Zhang and X. Zhou, *Chem. Commun.*, 2017, **53**, 11790–11793.
23 K. Jasuja and V. Berry, *ACS Nano*, 2009, **3**, 2358–2366.
24 D. Li, M. B. Müller, S. Gilje, R. B. Kaner and G. G. Wallace, *Nat. Nanotechnol.*, 2008, **3**, 101.
25 D. Luo, G. Zhang, J. Liu and X. Sun, *J. Phys. Chem. C*, 2011, **115**, 11327–11335.
26 P. Solis-Fernandez, M. Bissett and H. Ago, *Chem. Soc. Rev.*, 2017, **46**, 4572–4613.
27 J. Yang, R. Quhe, S. Feng, Q. Zhang, M. Lei and J. Lu, *Phys. Chem. Chem. Phys.*, 2017, **19**, 23982–23989.
28 S. Agnoli and M. Favaro, *J. Mater. Chem. A*, 2016, **4**, 5002–5025.
29 K. S. Novoselov, A. Mishchenko, A. Carvalho and A. H. Castro Neto, *Science*, 2016, **353**, aac9439.